Cytidine Derived Hydrogels with Tunable Antibacterial Activities

Article *in* ACS Applied Bio Materials · July 2019

DOI: 10.1021/acsabm.9b00438

6 authors, including:

Tanima Bhattacharyya
Indian Association for the Cultivation of Science
6 PUBLICATIONS **127** CITATIONS
SEE PROFILE

Ritapa Chaudhuri
Indian Association for the Cultivation of Science
6 PUBLICATIONS **67** CITATIONS
SEE PROFILE

Krishna Sundar Das
Indian Association for the Cultivation of Science
20 PUBLICATIONS **119** CITATIONS
SEE PROFILE

Jyotirmayee Dash
Indian Association for the Cultivation of Science
142 PUBLICATIONS **3,156** CITATIONS
SEE PROFILE

ACS APPLIED BIO MATERIALS

Cite This: ACS Appl. Bio Mater. 2019, 2, 3171−3177

Letter

www.acsabm.org

Cytidine-Derived Hydrogels with Tunable Antibacterial Activities

Tanima Bhattacharyya,[†] Ritapa Chaudhuri,[†] Krishna Sundar Das,[†] Raju Mondal,[†] Subhranshu Mandal,[‡] and Jyotirmayee Dash*[,†]

[†]School of Chemical Sciences, Indian Association for the Cultivation of Science, Jadavpur, Kolkata 700032, India

[‡]Calcutta Medical Research Institute, Kolkata 700027, India

Supporting Information

ABSTRACT: We herein report the preparation of hydrogels by the Ag^+ ion induced assembly of cytidine and boronic acids. These hydrogels, presumably formed by an *i*-motif like arrangement of cytidine and its boronate ester analogues, possess excellent thixotropic and self-healing properties. The hydrogels exhibit potent antimicrobial activity that can be tuned by varying the functional groups in their boronic acid component. These hydrogels could find potential use as antimicrobial agents and stimuli-responsive drug delivery systems.

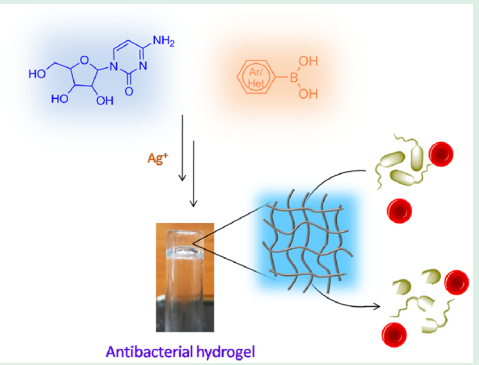

KEYWORDS: *antibacterial, cytidine, self-healing, silver acetate, stimuli responsive, thixotropic*

Supramolecular hydrogels composed of gelators having low molecular weight have found potential applications in drug delivery, sensing, catalysis, and tissue engineering.[1−4] Due to their reversible and modulable nature, these hydrogels have also emerged as interesting alternatives for the fabrication of antimicrobial materials that can be used in surgical dressings and in wound fillings.[5−9] These macromolecular systems have been considered as efficient antimicrobial agents because, unlike traditional antibiotics that act on intracellular targets without affecting the microbial morphology, these antibacterial hydrogel systems disrupt the microbial membrane of the bacteria.[9] Nucleosides, carbohydrates, and peptides are promising precursors for the construction of biocompatible supramolecular hydrogels.[10,11] They undergo self-assembly via noncovalent interactions like hydrogen bonding and $\pi-\pi$ interactions to form the hydrogel network.[10−15] Among nucleosides, the capability of guanosine to form gels by self-assembly has been well explored[11−15] since the first report by Bang et al. in 1910.[12] However, very few studies have focused on gel formation by self-assembly of other nucleosides.[15]

Besides guanosine, cytosine is also known to self-assemble via non-canonical hydrogen bonding and $\pi-\pi$ interactions to form an intercalated motif or the "*i*-motif".[16−20] Observed for the first time by Gehring, Leroy, and Guéron, the *i*-motif is a tetrameric structure composed of two parallel DNA duplexes held together in a head to tail pattern by intercalated hemiprotonated cytosine−cytosine base pairs.[16] The elementary unit of a *i*-motif structure is a base pair involving one protonated cytosine (positively charged at the N3 position) and one deprotonated (neutral) cytosine.[16−20]

Very recently, it has been shown that *i*-motif formation can be induced by Ag^+ cations at a physiological pH.[21−26] We herein report the preparation of hydrogels from the silver acetate stabilized assembly of cytidine (1) and arylboronic acids.[27] The hydrogels consisting of an *i*-motif like assembly of the cytidine and its boronate ester analogues show tunable antibacterial properties.

MATERIALS AND METHODS

Materials. Cytidine, boronic acids, silver acetate, crystal violet, rose bengal, XTT, PMS, kanamycin, and doxorubicin were purchased and used directly from the bottle. Autoclaved Milli-Q water with a pH of 7.4 was used in all experiments. The following bacterial strains were used: *Staphylococcus aureus* (ATCC 25923), *Pseudomonas aeruginosa* (ATCC 27853), *Escherichia coli* (ATCC 25922), *Streptococcus pneumoniae* (ATCC 49136), *Klebsiella pneumoniae* (human urine), and the multidrug-resistant strain of *Morganella morganii* (human urine). The *M. morganii* strain is resistant to drugs cefoperazone/sulbactum, levofloxacin, and minocycline.

Preparation of the Hydrogels. A 0.5 mL aqueous suspension of cytidine C (15 mg, 0.061 mmol), boronic acid, (0.061 mmol, 1.0 equiv), and silver acetate (4.5 mg, 0.030 mmol, 0.5 equiv) was heated at 50−60 °C until a clear solution was obtained. (Overheating resulted in a turbid solution that did not form efficient gels.) The resulting solution was then allowed to cool down to 30 °C and stored away from light. Gelation was slow and was observed after standing the solution for a period of 2 days at 30 °C and after a period of 5 days when incubated at temperatures lower than 30 °C. The

Received: May 24, 2019
Accepted: July 8, 2019
Published: July 8, 2019

DOI: 10.1021/acsabm.9b00438
ACS Appl. Bio Mater. 2019, 2, 3171−3177

Scheme 1. Formation of Cytidine−Boronic Acid Hydrogels by Self- Assembly of Dimers of Cytidine Derivatives

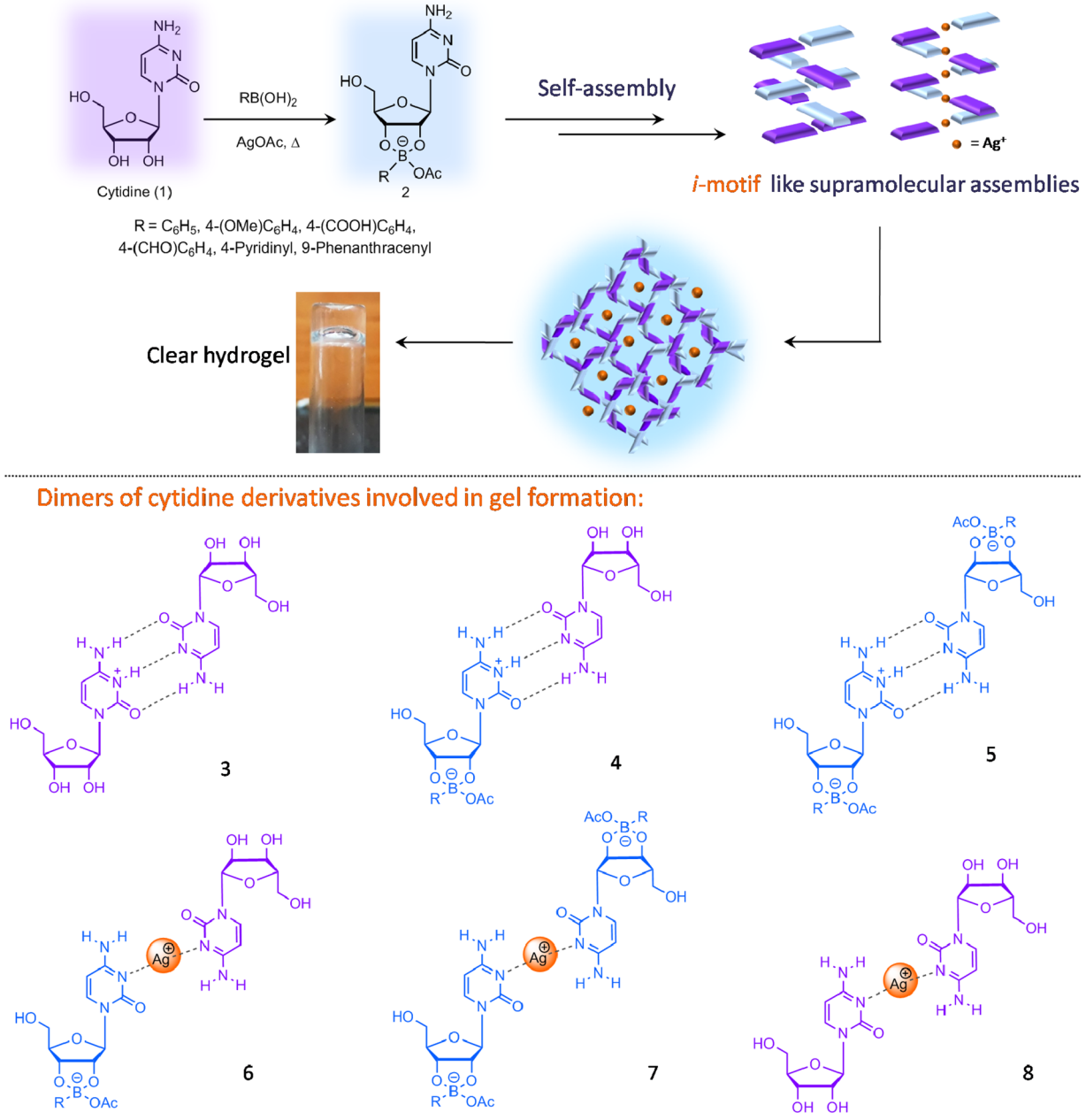

conditions for the formation of a stable hydrogel were optimized by varying the ratios of phenylboronic acid, cytidine, and silver acetate (Table S1).

Gels were also prepared with a variety of boronic acids (1:1:0.5 ratio of cytidine/boronic acid/silver acetate) to investigate the versatility of the process of gel formation. Gelation occurred with 4-formylphenylboronic acid, 4-methoxyphenylboronic acid, 4-carboxyphenylboronic acid, 9-phenanthracenylboronic acid, and 4-pyridinylboronic acid. The pH of these gels was found to be ∼5.5.

Determination of the Ionic Nature of the Hydrogel. Cytidine−phenylboronic acid hydrogels (0.5 mL each) were incubated with 100 μL of 10 mM rose bengal and crystal violet solutions, respectively, to observe selective absorption of dye by the hydrogel.

Self-Healing Properties of the Hydrogel. A block of a one month old hydrogel was cut into two pieces and kept in contact with each other in the absence of any external force.

Antimicrobial Activity. The antibacterial property of the hydrogel was assessed by determining the lowest concentration of the hydrogel, at which no visual growth of bacteria was observed or minimum inhibitory concentration (MIC); using broth microdilution assay. Antibacterial properties of the cytidine-derived hydrogels were determined against both Gram-positive (*S. aureus* and *S. pneumoniae*) and Gram-negative (*E. coli*, *P. aeruginosa*, *K. pneumoniae*, and *M. morganii*) bacteria. Different bacterial strains were cultured for 6 h in suitable media containing ∼10^9 CFU mL^{-1} (determined by the spread plating method). These were then further diluted to 10^5 CFU mL^{-1} using appropriate media. The standardized bacterial suspensions were then inoculated with increasing concentrations of the hydrogels along with those of the antimicrobial control kanamycin. The suspensions were then incubated at 37 °C for a period of 24 h and the OD values measured at 600 nm using a Multiscan FC ELISA reader (Thermo Scientific). The concentration of a respective hydrogel, for which no visible growth of bacteria was observed and the OD value was found to be nearest to the control, was considered as the MIC for that hydrogel. MIC values reported are an average of the data obtained from three independent experiments, and each experiment has been performed three times.

DOI: 10.1021/acsabm.9b00438
ACS Appl. Bio Mater. 2019, 2, 3171−3177

Cell Culture. Adult human normal kidney epithelial (NKE) cells were cultured using high-glucose media containing 10% FBS and 1% penicillin−streptomycin. Cells were expanded when they reached 70−80% confluency.

Cytotoxicity Analysis of the Different Cytidine Hydrogels. Cytotoxicities of different cytidine hydrogels in human normal kidney epithelial cells were evaluated using an XTT assay. The NKE cells were cultured at 37 °C in a 5% carbon dioxide (CO_2)/95% air atmosphere in tissue culture plates containing 4× 10^5 cells/well. XTT is a colorless or slightly yellow compound, which is metabolically reduced to give a bright orange color in live cells. The cells were then treated with different concentrations (5, 12.5, 25, 50, 100, and 500 μg/mL) of cytidine gel and incubated for 24 h. A solution (25 μL) containing 1 mg/mL of XTT and 3 mg/mL of PMS was added to 100 μL of the cell culture medium into each well. PMS was added to enhance the reduction reaction for better detection. The absorbance (A) of formazan dye was recorded at 450 nm using a microplate reader. The percentage of viable cells was determined by the following equation. IC_{50} values of the individual gel components were also calculated.

$$\text{viable cells (\%)} = \frac{\text{absorbance of treated cells}}{\text{absorbance of untreated cells}} \times 100$$

SEM Analysis of PBA Gel Treated *E. coli* Bacteria. *E. coli* was grown at mid log phase (0.5 McFarland standard) and incubated in the absence and presence of PBA gel at a concentration of 3 times the MIC value at standard culture conditions. The bacterial cells were then centrifuged at 5000 rpm for 3 min and washed two times with PBS buffer. Next, the bacteria were fixed with 2.5% glutaraldehyde at 4 °C for 1 h. They were then washed with PBS and dehydrated by washing in increasing concentrations of ethanol (50, 70, 80, 90, and 100% for 10 min) at room temperature. The samples were then drop casted on slides and then mounted on gold coated aluminum stubs. The changes in morphology of the *E. coli* cells were visualized using a FESEM (JEOL, JSM 6700F) operating at 1 kV.

Hemolytic Assay. The hemolytic activity of the cytidine hydrogel was determined against RBCs obtained from freshly drawn, heparinized human blood. Suspensions of human red blood cells were incubated with serial dilutions of the cytidine hydrogel. PBS buffer was used as negative hemolysis control and Triton X-100 (1% v/v) was used as positive hemolysis control. The plate was incubated at 37 °C for an hour and was then centrifuged at 3500 rpm for 5 min. 100 μL of the supernatant fluid was then put into a fresh micro titer plate and absorbance at 540 nm was recorded using a Multiscan FC ELISA reader (Thermo Scientific). The percentage of hemolysis was determined by the equation $(A - A_0)/(A_{total} - A_0) \times 100$, where A is the absorbance observed for the test well, A_0 the absorbance observed for the negative controls, and A_{total} the absorbance observed for 100% hemolysis wells, all at 540 nm. The HC_{50} values and errors reported are averages and standard errors of mean obtained from three independent experiments, respectively.

RESULTS AND DISCUSSION

The phenylboronic acid hydrogels were prepared by heating an aqueous suspension of cytidine (1 equiv), phenylboronic acid (1 equiv) and silver acetate (0.25−1 equiv) at 50−60 °C to obtain a transparent and colorless solution that was cooled down to 30 °C. Gelation was slow and was observed after standing the solution for a period of 2 days at 30 °C (Scheme 1, Figure S1; gelation was slower below 30 °C). A weak gel was obtained by using 0.25 equiv of Ag^+, while stronger gels were obtained on preparing gels with higher equivalents of Ag^+ (0.5, 0.75, and 1 equiv). While the gel prepared with 0.5 equiv of Ag^+ was clear and stable for several months; the gels prepared with 0.75 and 1.0 equivs of Ag^+ were not stable, and they began precipitating out within a month's time. The clear, self-supporting gel (PBA) formed with 0.5 equiv of Ag^+ was strong and stable when stored in the dark (Table S1). However, upon exposure to light, the gradual development of Ag nanoparticles within the gel matrix occurred due to the photochemical reduction of Ag^+ to Ag^0 with time (Figures S2 and S3). Gel formation was ensured using a conventional tube-inversion method. The pH of the gel formed was found to be 5.5.

Considering the pH of the gel, it can be presumed that some of the cytidine (**1**) or cytidine−boronate ester units (**2**) in the gel medium are protonated at the N3 position. The protonation of a cytosine (C) would have resulted in a C^+·C base pair with a nearby cytosine, and with time, the number of such pairs would have increased to provide fiber like assemblies. However, no gelation as a result of supramolecular assembly was observed at pH ∼ 5.5 by using only cytidine and phenylboronic acid, in the absence of silver ions. From this observation, it can be concluded that C·Ag^+·C base pairing in the presence of Ag^+ (**6**−**8**) plays a key role in the formation of the microstructure of the hydrogel. The presence of these species in the gel was confirmed from its MALDI-TOF spectrum (Figure S4). From the above observations, it can be stated that the C^+·C (**3**−**5**) and C·Ag^+·C (**6**−**8**) base pairs conjointly participate in the formation of the hydrogel. These base pairs stack upon one another, forming fiber like aggregations, which in turn entrap water within them to form the hydrogel. The formation of boronate esters, base pairing of cytidine analogues (**3**−**8**), and the organized alignment of the base pairs in the presence of silver ions presumably delay the gelation time. The gel assembly can be disintegrated by the addition of guanosine and cysteine. The disruption of the gel construct in the presence of guanosine may be due to the association of guanosine with cytidine at the cost of cytidine−cytidine base pairing. The cysteine-mediated disassembly of the gel network may be attributed to its ability to chelate and remove Ag^+.

The PBA gel was found to be highly pH sensitive. At pH ∼ 3, the gel assembly was disrupted, leading to precipitation. This may be attributed to the protonation of more cytidine units that disturbs the H-bonding between C and C^+. The gel assembly was also destroyed at pH values above 6.5, when the number of protonated cytosine bases is expected to reduce. The pH sensitivity of the hydrogel suggests the presence of the *i*-motif like supramolecular assembly of cytidine analogues within the hydrogel network. The formation of an *i*-motif like assembly within the hydrogel was further validated by the appearance of a positive signal at ∼287 nm and a negative signal at ∼264 nm, in the CD spectrum of the PBA hydrogel (Figure S5). Additionally, similar to the CD pattern of the DNA *i*-motif, the intensity of the first band was found to be greater than that of the second one.[16−26] From the PXRD pattern of the dried hydrogel, the stacking interval between the base pairs was found to be 3.1 Å (a broad peak at 28.6°) (Figure S2). This is similar to the stacking distance between C·C^+ pairs in DNA *i*-motif structures.[16−26]

The supramolecular cytidine gel (PBA) prepared was found to be thermoirreversible. Upon heating, water from the gel matrix evaporates, keeping the gel network intact to form xerogels. A thermogravimetric analysis (TGA) of the gel showed a major weight loss at ∼136.8 °C primarily because of the loss of the major constituent water from the medium of the PBA hydrogel (Figure S6). Another important observation was that the gelation occurred selectively with Ag^+ from CH_3COOAg. However, gelation was not observed with $AgNO_3$. No other cation like K^+, Cu^{2+}, Zn^{2+}, Mg^{2+}, Pb^{2+}, Hg^{2+}, etc. was found to induce a superassembly to form a gel. It

DOI: 10.1021/acsabm.9b00438
ACS Appl. Bio Mater. 2019, 2, 3171−3177

was also observed that no gel was formed by replacing phenylboronic acid with boric acid (H_3BO_3). Besides, no other nucleosides except cytidine could induce gelation. Since cytidine is highly soluble in water, base-pairing interactions between free cytidine and cytidine−boronate esters as well as $\pi-\pi$ stacking interactions of aryl rings are presumed to be the determining factors for the supramolecular architecture. The presence of boronate esters of cytidine in the hydrogel network was further confirmed by the absorption band at ∼1090 cm^{-1} ($\nu_{B\text{-}OC}$ for boronate esters) in the FTIR spectrum of the PBA xerogel (Figure S7).[28] To get detailed insight into the gelation phenomenon and structure−function relationship of the gelators, solution state NMR studies were carried out (Figure 1, Figure S8). Samples for NMR spectroscopy were prepared

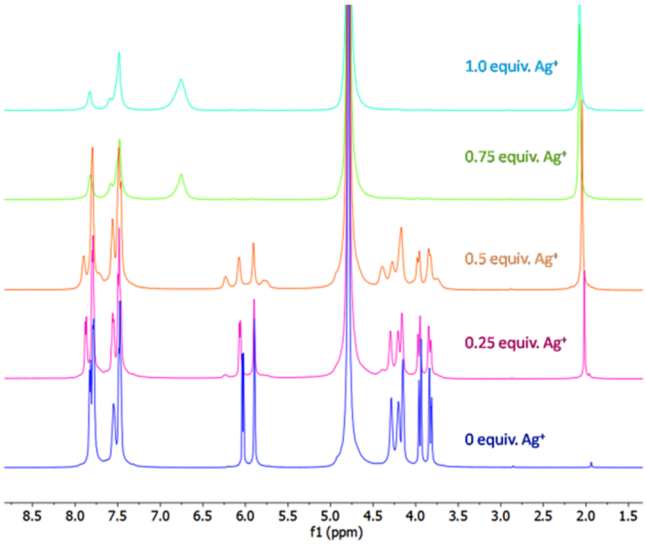

Figure 1. NMR spectra of the cytidine-derived hydrogels composed of different ratios of Ag^+.

by gel formation upon incremental addition of silver acetate to a constant concentration of cytidine and phenylboronic acid in D_2O. ^1H NMR spectra showed broadening of peaks with an increasing concentration of silver acetate. The integral values of the cytidine peaks were found to decrease with the progress in gelation. The NMR spectrum of the sample containing 0.25 equiv of silver acetate showed a gradual disappearance of peaks for C5 (∼5.8 ppm) and 1′H (∼5.7 ppm) protons of the free cytidine (**1**) along with gradual emergence of C5 (∼6.03 ppm) and 1′H (∼5.58 ppm) protons of the cytidine−boronate ester (**2**). The coexistence of these peaks was also observed in the NMR spectrum of the sample containing 0.5 equiv of silver acetate, the optimum condition for gel formation. Addition of silver acetate beyond this concentration led to almost complete disappearance of the cytidine−boronate ester peaks, while peaks for free cytidine were visible in a negligible amount. This indicates that the boronate ester moieties are no longer present in the gel medium and have mostly participated in the formation of gel fibers.

Selective absorption of cationic dyes like crystal violet over anionic dyes like rose bengal by the hydrogel demonstrates the anionic nature of the hydrogel due to the presence of anionic boronate esters (Figure S9). Rheological properties of cytidine−phenylboronic acid hydrogels with different molar ratios of silver were measured at 25 °C to understand the effect of the silver ion concentration on gel properties. The storage moduli (G') values of all of the gels measured as a function of % strain at a fixed frequency of 10 rad/s showed a substantial elastic response. The storage moduli (G') values were found to be greater than the loss moduli (G'') values, indicating the presence of a solid like viscoelastic hydrogel network. The storage modulus value was found to be increased with an increase in silver ion concentrations within the gel sample. The gel containing 0.25 equiv of Ag^+ showed a very low storage modulus value, while the comparatively unstable gels containing 0.75 and 1.0 equivs of Ag^+ showed much higher G' values as compared to the PBA gel containing 0.5 equiv of Ag^+, proving them to be much stronger gels than the PBA gel (Figure 2a).

The PBA hydrogel (synthesized with 0.5 equiv of Ag^+) exhibited a thixotropic property, which is an exceptional viscoelastic property. The gel underwent an isothermal, reversible gel to sol phase transition under physical stimuli like mechanical shaking and stirring, and again returned to its initial state upon standing. The thixotropic property of this gel was then studied by a continuous time sweep experiment under a sequential application of low strain (0.05%) and high strain (100%) conditions, separated by a time gap to ensure the complete gel-to-sol ($G' > G''$) and sol-to-gel ($G'' > G'$) conversion (Figure 2b). In the first step, when a low 0.05% strain was applied, the gel retained its properties. In the second step, the gel was completely broken down upon application of a high 100% strain and again returned to the gel state at a low strain (0.05%), in the next step. The destruction and recovery process could be repeatedly performed to determine the ability of the PBA gel to restore the mechanical properties. The rheological studies were performed at a constant angular frequency of 10 rad/s.

The thixotropic nature of the hydrogel has also been established by a detailed investigation of the morphology of the hydrogel using AFM and TEM techniques. The presence of a highly entangled three-dimensional network of thin thread like fibers in the hydrogel matrix was observed in the AFM and TEM images of the hydrogel (Figure 2c−f). The formation of nanoparticles on the gel fibers upon exposing the gel to light for 2 days can also be observed in the TEM image of the PBA hydrogel (Figure 2d). The average diameter of the fibers in the gel matrix was found to be around 10 nm. The average height of the gel fibers calculated from their AFM images was found to be 8.1 nm (Figure 2e,f). The AFM image of the gel subjected to mechanical distress showed the presence of broken discontinuous fibers (Figure 3b). Again, the AFM image of the same destroyed gel upon standing for ∼15 min revealed the presence of long continuous fibers as were previously present in the intact gel (Figure 2e).

The native cytidine hydrogel (PBA) also showed an interesting self-healing property. Two different slices of gel when kept in contact with each other (in the absence of any kind of external force) joined together to form a single block after a resting time of about 2 days (Figure 3c). This block formed by self-healing of the gel could be easily lifted without breaking.

Thixotropy and regenerative properties of supramolecular materials have drawn enormous attention from the industry and academia in recent days.[2,3,7,15] Hydrogels with such properties have been used in several biological applications like drug delivery and cell culture and as regenerative medicine, which can promote tissue healing after injuries and diseases.[2,3,7,15] Thus, the PBA hydrogel can be used as a

DOI: 10.1021/acsabm.9b00438
ACS Appl. Bio Mater. 2019, 2, 3171−3177

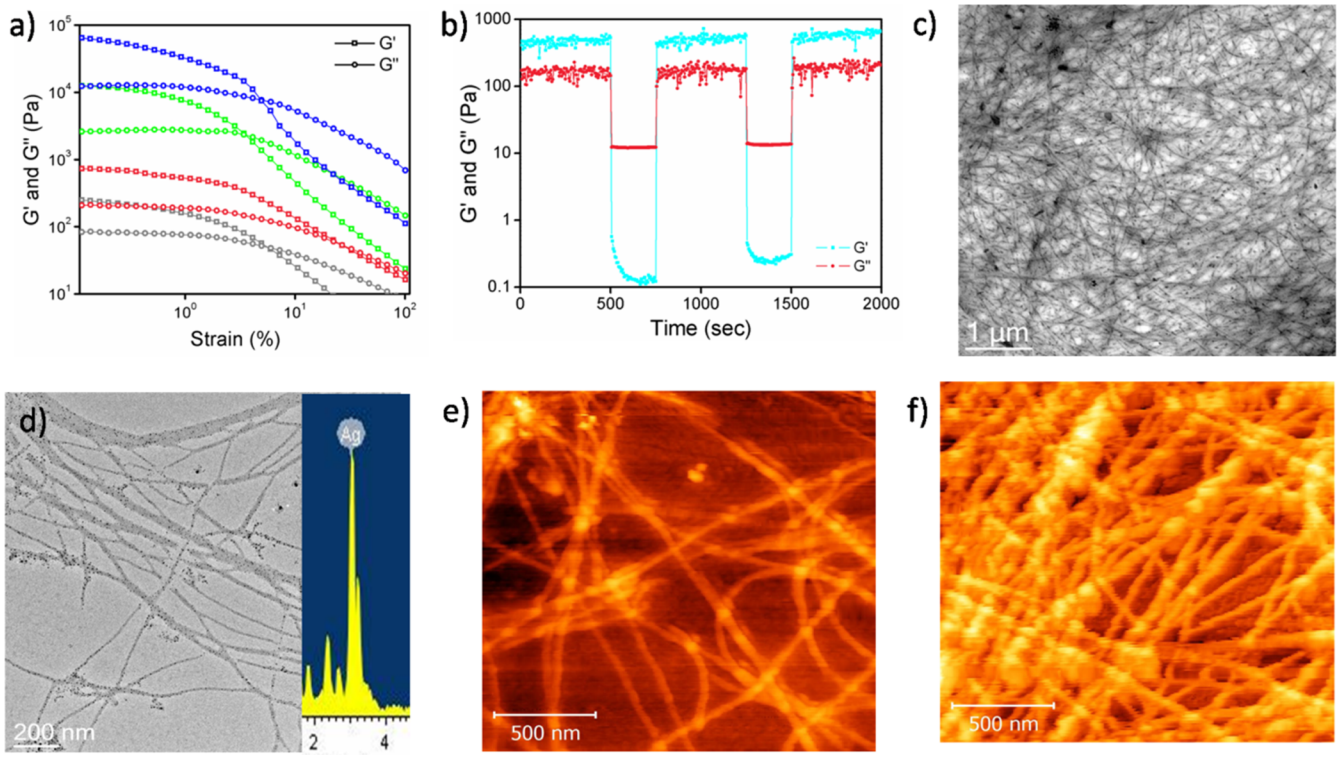

Figure 2. (a) Strain-dependent rheology measurement of the cytidine−phenylboronic acid hydrogels containing 0.25 equiv of Ag^+ (ash), 0.5 equiv of Ag^+ (red), 0.75 equiv of Ag^+ (green), and 1.0 equiv of Ag^+ (blue) with a strain sweeping from 0.05 to 100% at an angular frequency of 10 rad/s. (b) A measurement of the thixotropic property of the PBA hydrogel by a continuous step strain measurement in the presence of an alternative strain of 0.05% and 100%, respectively, with time at a constant angular frequency of 10 rad/s. (c) TEM image showing thread like nanostructure present within the PBA gel. (d) TEM image of the hydrogel after 2 days of exposure to light, showing the presence of Ag nanoparticles on the gel fibers (inset shows the corresponding EDX spectrum). (e) AFM image of the same hydrogel. (f) AFM image of the hydrogel after 2 days of exposure to light, showing the presence of Ag nanoparticles on the gel fibers.

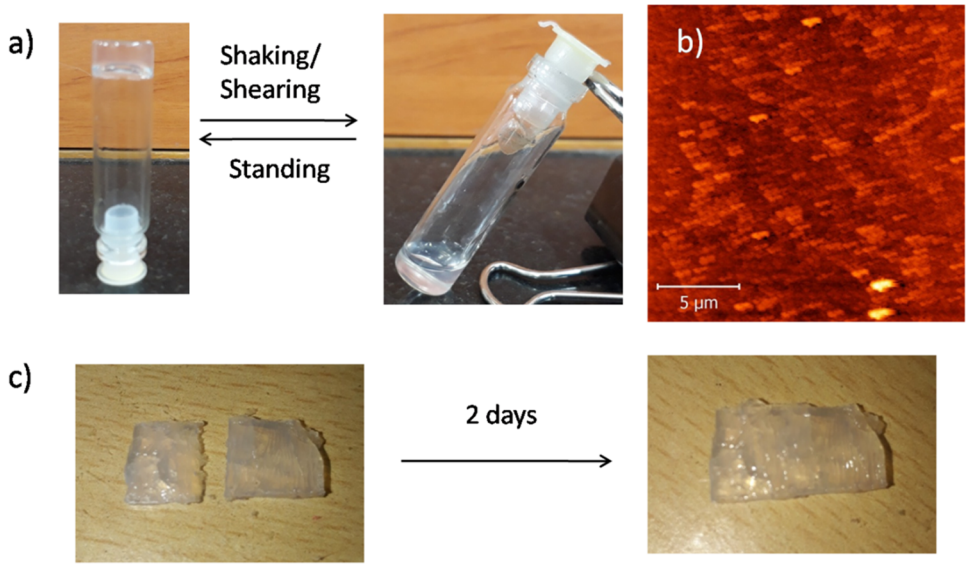

Figure 3. (a) Destruction and recovery of the gel by mechanical stress. (b) AFM image of the hydrogel destroyed under an application of stress. (c) Self-healing nature of the hydrogel.

vector in drug delivery applications.[29] The pH sensitive nature of the hydrogel can also be exploited to prepare a pH responsive drug delivery vehicle.[29] We have shown that doxorubicin, a potent anticancer drug, can be imbibed into the PBA hydrogel and then released by disrupting the gel assembly using external stimuli like mechanical shearing and change in pH (Figure S10).

Moreover, we have demonstrated that the PBA hydrogel exhibits promising antibacterial activity against Gram-negative bacterial strains like *E. coli*, *P. aeruginosa*, *K. pneumoniae*, and the multidrug resistant strain *M. morganii* and to a fair extent

DOI: 10.1021/acsabm.9b00438
ACS Appl. Bio Mater. 2019, 2, 3171−3177

Table 1. IC_{50} and MIC Values (μg/mL) of Hydrogels

		MIC values[b]					
		Gram-positive bacteria		Gram-negative bacteria			
boronic acid gels[a]	IC_{50}[b] (μg/mL)	*S. aureus*	*S. pneumoniae*	*E. coli*	*P. aeruginosa*	*K. pneumoniae*	*M. morganii*
PBA	182.42	50	50	10	10	20	40
For-PBA	81.19	75	100	20	10	50	40
Py-BA	200.34	>500	200	15	15	30	45
Carb-PBA	30.02	500	200	20	25	45	50
Met-PBA	43.98	100	100	75	50	50	50
Phen-BA	35.77	200	100	15	25	25	25

[a]Gels prepared from different boronic acids: PBA= phenylboronic acid gel, For-PBA= 4-formylphenylboronic acid gel, Py-BA= 4-pyridinylboronic acid gel, Carb-PBA= 4-carboxyphenylboronic acid gel, Met-PBA= 4-methoxyphenylboronic acid gel, Phen-PBA= 9-phenanthracenylboronic acid gel. [b]The concentration of gels has been calculated in terms of their cytidine content.

against Gram-positive bacterial strains like *S. aureus* and *S. pneumoniae* (Table 1). The in vitro antimicrobial activity of the PBA hydrogel was evaluated by determining its minimum inhibitory concentration (MIC), that is, the minimum concentration of compounds required to completely inhibit the growth of bacteria. The MIC values for the individual components were also evaluated. It was observed that MIC values for cytidine and phenylboronic acid were very high (>500 μg/mL) against all strains. Silver acetate, which is known for its antibacterial property,[30] showed a comparable MIC value (~50 μg/mL) with respect to that of the gel.

Next, the cytotoxic effects of the hydrogel and its individual components on human normal kidney epithelial (NKE) cells were evaluated by an XTT assay. Interestingly, it was observed that, although silver acetate was toxic (IC_{50} ~ 35 μg/mL), the PBA hydrogel impregnated with silver acetate was almost nontoxic exhibiting IC_{50} values much higher than the optimum dose, in which it exhibited antibacterial properties. The PBA gel displayed an IC_{50} value (182.42 μg/mL) almost 18-fold higher than its MIC values observed for Gram-negative strain *E. coli*. Thus, this manifests that the gel can serve as an efficient biocompatible silver containing formulation for antibacterial applications. Scanning electron microscopy (SEM) was carried out to determine the effect of the PBA hydrogel on the morphologies of the *E. coli* cells. The untreated *E. coli* cells showed a normal cellular morphology with smooth cell surfaces. On the other hand, the PBA hydrogel treated cells exhibited a reduction in cell size as well as cell membrane disruptions. The observed aggregation in the image of the treated cells is possibly due to the leakage of cellular contents upon disruption of the bacterial cell membrane (Figure 4).

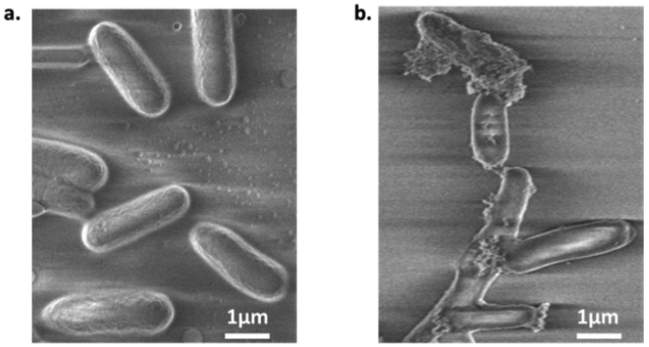

Figure 4. (a) SEM image of the untreated *E. coli* bacterial cells. (b) SEM image of *E. coli* bacterial cells after treatment with PBA gel.

We then intended to determine whether introduction of functional groups within the gel network would affect its antibacterial property. Gel formation was carried out with a wide variety of functionalized boronic acids, but gels were formed only with 4-formylphenylboronic acid, 4-methoxyphenylboronic acid, 4-carboxyphenylboronic acid, 9-phenanthracenylboronic acid, and 4-pyridinylboronic acid.

Unlike the phenylboronic acid gel (PBA gel), these gels showed selective antibacterial activity. These gels with functionalized boronic acids showed potent antibacterial activity toward Gram-negative strains like *P. aeruginosa*, *E. coli*, *K. pneumoniae*, and multidrug resistant *M. morganii*, whereas they were considerably inefficient against Gram-positive strains with a rigid cell wall composed of peptidoglycan. They showed MIC values ranging between 10 and 75 μg/mL for Gram-negative strains, while MICs $\geq$ 75 μg/mL were exhibited for Gram-positive *S. aureus* and *S. pneumoniae* strains. This demonstrates a synergistic antibacterial effect of gel components.

Hemolysis experiments established that the hydrogels are nontoxic to human erythrocytes at concentrations where antimicrobial behavior is observed (Figure S12). For instance, the PBA hydrogel showed negligible hemolysis (<5%) at a concentration higher than the MIC values for *E. coli* and *P. aeruginosa*. It showed merely 41% hemolysis at a hydrogel concentration of 500 μg/mL, which is many fold higher than the MIC values.

CONCLUSION

In conclusion, we have demonstrated the preparation of biocompatible hydrogels by the silver ion driven *i*-motif like supramolecular assembly of cytidine and its boronate ester derivatives. The hydrogels are easily synthesizable, exhibiting excellent thixotropic and self-healing properties. These hydrogels show potent antibacterial activities, and their selectivity toward Gram-negative bacteria has been enhanced by altering their boronic acid component. We believe that this gel system composed of a synergistic combination of silver with boronate esters may prove to be useful for devising next-generation antibiotics to fight against multidrug resistance.[5−9] Moreover, as this gel system contains silver acetate, it would not stain the skin tissues at the application site. This property renders it advantageous over other antibacterial gels containing silver nitrate. The scope of this hydrogel platform against other microbial species is currently under investigation.

DOI: 10.1021/acsabm.9b00438
ACS Appl. Bio Mater. 2019, 2, 3171−3177

■ ASSOCIATED CONTENT

Supporting Information

The Supporting Information is available free of charge on the ACS Publications website at DOI: 10.1021/acsabm.9b00438.

Additional experiments, standardization and characterization data of gels, and hemolytic and cytotoxicity analysis data of the hydrogels (PDF)

■ AUTHOR INFORMATION

Corresponding Author

*E-mail: ocjd@iacs.res.in. Fax: +91-33-2473-2805. Tel: +91-33-2473-4971, extension 1405.

ORCID

Raju Mondal: 0000-0002-9013-7259

Jyotirmayee Dash: 0000-0003-4130-2841

Notes

The authors declare no competing financial interest.

■ ACKNOWLEDGMENTS

The authors thank DST, India for funding. J.D. thanks DST for a SwarnaJayanti fellowship. T.B. thanks CSIR-India for a research fellowship. R.C. thanks UGC for a research fellowship. K.S.D. thanks DST-INSPIRE for a research fellowship.

■ ABBREVIATIONS

PBA, phenylboronic acid gel; For-PBA, 4-formylphenylboronic acid gel; Py-BA, 4-pyridinylboronic acid gel; Carb-PBA, 4-carboxyphenylboronic acid gel; Met-PBA, 4-methoxyphenylboronic acid gel; Phen-PBA, 9-phenanthracenylboronic acid gel

■ REFERENCES

(1) Hirst, A. R.; Escuder, B.; Miravet, J. F.; Smith, D. K. High-tech applications of self-assembling supramolecular nanostructured gel-phase materials: from regenerative medicine to electronic devices. *Angew. Chem., Int. Ed.* **2008**, *47*, 8002−8018.

(2) Du, X. W.; Zhou, J.; Shi, J. F.; Xu, B. Supramolecular hydrogelators and hydrogels: from soft matter to molecular biomaterials. *Chem. Rev.* **2015**, *115*, 13165−13307.

(3) Tang, J. D.; Mura, C.; Lampe, K. J. A stimuli-responsive, pentapeptide, nanofiber hydrogel for tissue engineering. *J. Am. Chem. Soc.* **2019**, *141*, 4886−4899.

(4) Qian, X.; Stadler, B. Recent developments in polydiacetylene-based sensors. *Chem. Mater.* **2019**, *31*, 1196−1222.

(5) Li, P.; Poon, Y. F.; Li, W.; Zhu, H.-Y.; Yeap, S. H.; Cao, Y.; Qi, X.; Zhou, C.; Lamrani, M.; Beuerman, R. W.; Kang, E.-T.; Mu, Y.; Li, C. M.; Chang, M. W.; Jan Leong, S. S.; Chan-Park, M. B. A polycationic antimicrobial and biocompatible hydrogel with microbe membrane suctioning ability. *Nat. Mater.* **2011**, *10*, 149−156.

(6) Ng, V. W. L.; Chan, J. M. W.; Sardon, H.; Ono, R. J.; Garcia, J. M.; Yang, Y. Y.; Hedrick, J. L. Antimicrobial hydrogels: a new weapon in the arsenal against multidrug-resistant infection. *Adv. Drug Delivery Rev.* **2014**, *78*, 46−62.

(7) Griffin, D. R.; Weaver, W. M.; Scumpia, P. O.; Di Carlo, D.; Segura, T. Accelerated wound healing by injectable microporous gel scaffolds assembled from annealed building blocks. *Nat. Mater.* **2015**, *14*, 737−744.

(8) Hu, B.; Owh, C.; Chee, P. L.; Leow, W. R.; Liu, X.; Wu, Y.-L.; Guo, P.; Loh, X. J.; Chen, X. Supramolecular hydrogels for antimicrobial therapy. *Chem. Soc. Rev.* **2018**, *47*, 6917−6929.

(9) Tang, Q.; Plank, T.; Zhu, T.; Yu, H.; Ge, Z.; Li, Q.; Li, L.; Davis, J. T.; Pei, H. Self-assembly of metallo-nucleoside hydrogels for injectable materials that promote wound closure. *ACS Appl. Mater. Interfaces* **2019**, *11*, 19743−19750.

(10) Sivakova, S.; Rowan, S. J. Nucleobases as supramolecular motifs. *Chem. Soc. Rev.* **2005**, *34*, 9−21.

(11) Peters, G. M.; Davis, J. T. Supramolecular gels made from nucleobase, nucleoside and nucleotide analogs. *Chem. Soc. Rev.* **2016**, *45*, 3188−3206.

(12) Bang, I. Untersuchungen über die Guanylsäure. *Biochem. Z.* **1910**, *26*, 293−311.

(13) Lena, S.; Masiero, S.; Pieraccini, S.; Spada, G. P. Guanosine hydrogen-bonded scaffolds: a new way to control the bottom-up realisation of well-defined nanoarchitectures. *Chem. - Eur. J.* **2009**, *15*, 7792−7806.

(14) Bhattacharyya, T.; Saha, P.; Dash, J. Guanosine-derived supramolecular hydrogels: recent developments and future opportunities. *ACS Omega* **2018**, *3*, 2230−2241.

(15) Pu, F.; Ren, J.; Qu, X. Nucleobases, nucleosides and nucleotides: versatile biomolecules for generating functional nanomaterials. *Chem. Soc. Rev.* **2018**, *47*, 1285−1306.

(16) Guéron, M.; Leroy, J.-L. The *i*-motif in nucleic acids. *Curr. Opin. Struct. Biol.* **2000**, *10*, 326−331.

(17) Day, H. A.; Pavlou, P.; Waller, Z. A. *i*-Motif DNA: structure, stability and targeting with ligands. *Bioorg. Med. Chem.* **2014**, *22*, 4407−4418.

(18) Benabou, S.; Aviñó, A.; Eritja, R.; González, C.; Gargallo, R. Fundamental aspects of the nucleic acid *i*-motif structures. *RSC Adv.* **2014**, *4*, 26956−26980.

(19) Dong, Y.; Yang, Z.; Liu, D. DNA nanotechnology based on *i*-motif structures. *Acc. Chem. Res.* **2014**, *47*, 1853−1860.

(20) Mergny, J. L.; Sen, D. DNA quadruple helices in nanotechnology. *Chem. Rev.* **2019**, *119*, 6290−6325.

(21) Ono, A.; Cao, S.; Togashi, H.; Tashiro, M.; Fujimoto, T.; Machinami, T.; Oda, S.; Miyake, Y.; Okamoto, I.; Tanaka, Y. Specific interactions between silver (I) ions and cytosine-cytosine pairs in DNA duplexes. *Chem. Commun.* **2008**, *39*, 4825−4827.

(22) Urata, H.; Yamaguchi, E.; Nakamura, Y.; Wada, S.-i. Pyrimidine-pyrimidine base pairs stabilized by silver (I) ions. *Chem. Commun.* **2011**, *47*, 941−943.

(23) Day, H. A.; Huguin, C.; Waller, Z. A. Silver cations fold *i*-motif at neutral pH. *Chem. Commun.* **2013**, *49*, 7696−7698.

(24) Berdakin, M.; Steinmetz, V.; Maitre, P.; Pino, G. A. Gas phase structure of metal mediated (cytosine) $2Ag^{+}$ mimics the hemiprotonated (cytosine) $2H^{+}$ dimer in *i*-motif folding. *J. Phys. Chem. A* **2014**, *118*, 3804−3809.

(25) Fortino, M.; Marino, T.; Russo, N. Theoretical study of silver-ion-mediated base pairs: the case of C-Ag-C and C-Ag-A systems. *J. Phys. Chem. A* **2015**, *119*, 5153−5157.

(26) Espinosa Leal, L. A.; Karpenko, A.; Swasey, S.; Gwinn, E. G.; Rojas-Cervellera, V.; Rovira, C.; Lopez-Acevedo, O. The role of hydrogen bonds in the stabilization of silver-mediated cytosine tetramers. *J. Phys. Chem. Lett.* **2015**, *6*, 4061−4066.

(27) Dash, J.; Bhattacharyya, T.; Chaudhuri, R. Nucleoside Hydrogels with Antibacterial Properties. *Indian Patent*. 201931025092, June 24, 2019.

(28) Bhattacharyya, T.; Kumar, Y. P.; Dash, J. Supramolecular hydrogel inspired from DNA structures mimics peroxidase activity. *ACS Biomater. Sci. Eng.* **2017**, *3*, 2358−2365.

(29) Li, J.; Mooney, D. J. Designing hydrogels for controlled drug delivery. *Nat. Rev. Mater.* **2016**, *1*, 16071−16088.

(30) Clement, J. L.; Jarrett, P. S. Antibacterial silver. *Met.-Based Drugs* **1994**, *1*, 467−482.

DOI: 10.1021/acsabm.9b00438
ACS Appl. Bio Mater. 2019, 2, 3171−3177